Imaging and Radiation Research (2019) Volume 2 Issue 1
doi:10.24294/irr.v2i1.1720

ORIGINAL RESEARCH ARTICLE

A dual-model-based inversion method for integrated aperture radiometer imaging

Jianfei Chen[1,2*], Li Zhu[2], Yuehua Li[2]

[1*] *School of Electronic and Optical Engineering, Nanjing University of Posts and Telecommunications, Nanjing 210003, Jiangsu province, China. E-mail: chenjf@ njupt.edu.cn*

[2] *School of Electronic Engineering and Optoelectronic Technology, Nanjing University of Science and Technology, Nanjing 210094, Jiangsu province, China.*

ABSTRACT

To address the problem that the imaging inversion method based on a single model in integrated aperture imaging is difficult to effectively correct model errors and perform accurate image reconstruction, a dual-model (DM)-based integrated aperture imaging inversion method is proposed for correcting the parametric errors of the inversion model and performing highly accurate millimeter-wave image reconstruction of the target scene. In view of the different parameter sensitivities of the Fourier transform (MFFT) model and the G-matrix (GM) model, the proposed DM method first corrects the imaging parameters with errors accurately by comparing the reconstruction errors of the two models; then recon-structs a high-precision target image based on the accurate GM model with the help of an improved regularization method. It is proved by simulation experiments that the proposed DM method can effectively correct the parameter errors of the imaging model and reconstruct the target scene with high accuracy in millimeter wave images com-pared with the traditional single-model imaging method.

Keywords: Millimeter Wave; Integrated Aperture; Radiometer; Imaging Method; Regularization

ARTICLE INFO

Received: 12 September 2019
Accepted: 28 November 2019
Available online: 17 December 2019

1. Introduction

Millimeter-wave synthetic aperture interferometric radiometer (SAIR) breaks the limitation of antenna aperture on spatial resolution with the help of integrated aperture technology, and can achieve high-resolution imaging detection using small-aperture array antennas; it also has the characteristics of both infrared and microwave imaging, and can penetrate clothing, plastic, wood and other materials to achieve high-precision stealth detection, and has been widely used in military, navigation, medical and traffic security monitoring[1-3]. However, due to some unavoidable factors (such as background noise, system parameters and imaging model errors), like other non-optical imaging systems, the image reconstructed by SAIR is a degraded image, and there is a certain error between it and the real millimeter wave image. At present, typical SAIR imaging methods (such as MFFT, NUFFT, Gridding, and regularized inversion methods) are used to optimally reconstruct the target scene under their own inversion models with the help of numerical inversion, and their reconstruction accuracy largely depends on the accuracy of the adopted inversion models[4-7]. However, due to some simplifying approximations in the model construction, the actual SAIR inversion model often suffers from certain description errors. In addi-

tion, some imaging parameters are often difficult to obtain accurately due to specific environmental constraints in practical imaging applications. In this case, it is difficult to reconstruct an accurate millimeter wave image with the help of the above-mentioned traditional imaging method based on a single model.

At present, the Fourier transform (MFFT) model and the G-matrix (GM) model are two typical high-precision imaging models for SAIR imaging inversion. Among them, the GM model has higher model accuracy and can reconstruct high precision millimeter wave images; however, its parameter sensitivity is high and inaccurate model parameters will lead to higher inversion errors. The MFFT model, on the other hand, has lower model accuracy and parameter sensitivity, and is an inert imaging model; its reconstructed image accuracy is lower but more stable. With the model parameters approximating the exact parameters, the reconstructed images of both models are close to the real millimeter wave images, and the reconstruction errors between the two models are minimized. In order to make full use of the advantages of both models and perform highly refined reconstruction of the real millimeter-wave images, an integrated aperture inversion method based on the dual imaging model (DM) is proposed in this paper. The proposed DM method first corrects the imaging parameters with errors by comparing the reconstruction errors between the GM model and the MFFT model, and then improves the model accuracy of the imaging model; then, the inert MFFT model is used to constrain the inversion process of the GM model with the help of the reconstructed image of the inert MFFT model, and the improved regularization method is used to reconstruct the target scene with high accuracy. The simulation results show that the proposed DM method can effectively correct the parametric errors of the imaging model and achieve high-precision reconstruction recovery of the millimeter wave image of the target scene compared with the traditional single-model imaging method.

2. Millimeter-wave SAIR imaging model

Before introducing the DM inversion method, the MFFT and GM models are first briefly explained in conjunction with **Figure 1**. The array antenna is located in the *OXY* plane, the target is located in the *oxy* plane, and the distance between the *i*-th radiation source *Si* and antennas *c* and *l* are R_i^c and R_i^l after target discretization, respectively.

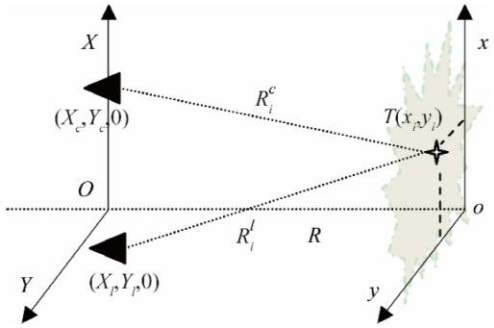

Figure 1. Integrated aperture imaging geometry.

Based on the interferometric principle of the integrated aperture radiometer, a sample of the visibility function measured by the antenna for (*c*, *l*) can be expressed as:

$$V_{c,l} = \langle E_c(R_i^c, t) \cdot E_l^*(R_i^l, t) \rangle_\tau = \sum_{i=1}^{N} T(x_i, y_i) F_c(x_i, y_i) F_l^*(x_i, y_i) r_{c,l} e^{-jk(R_i^c - R_i^l)} \tag{1}$$

where, $E_{\#}(\cdot)$ is the electromagnetic signal received by the array antenna, $\langle\cdot\rangle$ denotes the time integration, τ is the integration time, (x_i,y_i) is the S_i coordinates, $T(x_i,y_i)$ is the normalized bright temperature, $F_{\#}(\cdot)$ is the antenna orientation map, $k = 2\pi/\lambda$ is the circular wave number, λ is the system center wavelength, $r_{c,l}$ is the striation function. $\exp[-jk(R_i^c - R_i^l)]$ denotes the phase difference between antenna pairs (*c*,*l*). In the MFFT model, a Taylor approximation expansion is often performed for R_i^c and R_i^l:

$$R_i^c \approx R + [(x_i - X_c)^2 + (y_i - Y_c)^2]/2R \tag{2}$$

$$R_i^l \approx R + [(x_i - X_l)^2 + (y_i - Y_l)^2]/2R \tag{3}$$

Substituting equations (2) and (3) into equation (1) and defining $u = k(X_l - X_c)/$, $v = k(Y_l - Y_c)/R$, we can get:

$$V(u,v) = e^{-j\varphi(u,v)} \iint T(x,y) F_c F_l^* r_{c,l} e^{-j(xu+yv)} dxdy \tag{4}$$

where, $\varphi(u,v) = \pi(X_c^2 + Y_c^2 - X_l^2 - Y_l^2)/\lambda R$ is the phase compensation term, which can effec-

tively improve the near-field imaging accuracy of SAIR. For ideal SAIR, $r_{c,l}$ and the antenna orientation map $F_{\#}(\cdot)$ can be further approximated as 1, and equation (4) can be written as the following MFFT imaging model:

$$V(u,v) = e^{-j\varphi(u,v)} \iint T^{\mathrm{MF}}(x,y) e^{-j(xu+yu)} dxdy \tag{5}$$

$$T^{\mathrm{MF}}(x,y) = FT_2\left[V(u,v)^{\mathrm{j}\varphi(u,v)}\right] \tag{6}$$

The above equation is the MFFT imaging model, T^{MF} is an approximation of the real image T, and $FT_2[\cdot]$ is the two-dimensional Fourier transform. The MFFT imaging method is based on equation (6) to reconstruct the target image by the fast Fourier transform. Due to the high stability of the Fourier transform operation, the reconstructed images T^{MF} of the MFFT method are relatively stable, but the reconstructed images T^{MF} have large errors relative to the actual millimeter wave images T due to the low accuracy of the MFFT model.

For a more accurate model description of the integrated aperture imaging process, R_i^c and R_i^l can be precisely represented according to **Figure 1** as:

$$R_i^c = \sqrt{(x_i - X_c)^2 + (y_i - Y_c)^2 + R^2} \tag{7}$$

$$R_i^l = \sqrt{(x_i - X_l)^2 + (y_i - Y_l)^2 + R^2} \tag{8}$$

Substituting equations (7) and (8) into equation (1), the following matrix equation can be derived.

$$V_{M\times 1} = G_{M\times N} \cdot T_{N\times 1} \tag{9}$$

$$G(m,n) = F_{mc}(x_i,y_i) F_{ml}^*(x_i,y_i) \cdot e^{j\frac{2\pi}{\lambda}\left[\sqrt{(x_i-X_{ml})^2+(y_i-Y_{ml})^2+R^2}-\sqrt{(x_i-X_{mc})^2+(y_i-Y_{mc})^2+R^2}\right]} \tag{10}$$

Equation (9) is the exact GM model, which describes the SAIR imaging process more accurately than the MFFT model of approximate description; therefore, the accuracy of the reconstructed images T^{G} based on the GM model is significantly higher than the results T^{MF} of the MFFT model.

In the actual millimeter wave SAIR, the measured visibility function often has a certain observation error, and the number of sampling points M is usually much smaller than the number of pixels N to be recovered; at this time, the accurate inverse solution of equation (9) can be performed with the help of the regularization method, and the typical reconstruction model is:

$$min_T J(\boldsymbol{T}) = \|\boldsymbol{GT} - \boldsymbol{V}\|_2^2 + \alpha\|\boldsymbol{CT}\|_2^2 \tag{11}$$

where $\|\boldsymbol{GT} - \boldsymbol{V}\|_2^2$ is the fidelity term to ensure that the difference between the reconstructed image and the real millimeter-wave image is small enough, $\|\boldsymbol{CT}\|_2^2$ is the regularization term, and α is the regularization parameter, and α is often set as small as possible to maintain the high resolution of the millimeter-wave image.

3. Integrated aperture inversion method based on dual model

From the above analysis, it can be seen that the model accuracy of the GM model is high, but the parameter sensitivity is high, and inaccurate model parameters will lead to high reconstruction errors. In practical applications, some imaging parameters are often difficult to be accurately determined, and at this time, accurate millimeter wave images cannot be reconstructed with the help of the GM model. While the MFFT model has lower reconstruction accuracy, its reconstructed image has high stability and is an inert imaging model. Combining the characteristics of the two models, this paper proposes an integrated aperture inversion method based on the dual model (DM). Firstly, the error correction of imaging parameters is performed by comparing the reconstruction errors between the GM and MFFT models; then the improved regularization method is used to reconstruct the target scene with high accuracy.

3.1 Model parameter correction

By comparing the two imaging models, it can be seen that the main model parameters are R, λ and antenna position ($X_{\#}$, $Y_{\#}$), etc. Compared with other parameters, the GM model is extremely sensitive to the parameters R; and the distance R is sometimes difficult to be determined accurately due

to environmental constraints. Therefore, in this paper, the parameter calibration process of the DM method is illustrated with the parameters R as an example.

(1) The image inversion is performed with the help of MFFT model and GM model respectively within the confidence interval of R (usually $0.5R_0 \sim 1.5R_0$, R_0 is the predicted imaging distance).

(2) Calculate the root mean square error RMSE between the inverse images of the two models; and plot the variation curve of RMSE with the parameter R. The RMSE is calculated as follows.

$$\mathrm{RMSE}(T,T_0)=\sqrt{\sum_i\left[T(i)-T_0(i)\right]^2}\Big/\sqrt{\sum_i\left[T_0(i)\right]^2} \tag{12}$$

where T_0 is the reference image, and T is the reconstructed image to be evaluated.

(3) Find the minimum value in the RMSE curve, and its corresponding R is the accurate value parameter R_a to be corrected.

The following is a set of simulation experiments to analyze the performance of the parameter correction method visually, and the main simulation parameters are shown in **Table 1**.

Table 1. Main simulation parameters

Parameter	Center wavelength λ/mm	Number of array element antennas	Antenna spacing Δd/m	Imaging distance R/m
Numerical value	8	100	0.01	500

The 100 array elements antennas were arranged into a line array with an antenna spacing of 0.01m. After the visibility function is obtained using electromagnetic simulation, the target scene T^A is reconstructed using the MFFT method and the GM-based regularization method respectively, and the corresponding simulation results are shown in **Figure 2**. From **Figure 2a**, it can be seen that the RMSE(T^{MF}, T^A) of the MFFT reconstructed result remains basically unchanged as the distance parameter R changes, while the RMSE(T^G, T^A) of the GM model changes more drastically due to the high sensitivity of the parameters, and only has a high reconstruction accuracy around R_a = 500 m. This indicates that the reconstruction accuracy of the GM model is better than that of the MFFT model under the accurate parameter settings (as shown in **Figure 2b**); however, when there are errors in the parameters, the GM model will not be able to perform accurate image reconstruction. In addition, the error curves RMSE(T^G, T^{MF}) and RMSE(T^G, T^A) curves between the two models are very similar and all reach the minimum at R_a. This indicates that even if the real image T^A is not known, the exact parameter R_a can be found based on RMSE(T^G, T^{MF}). From the error curves about the parameters λ given in **Figure 2c**, it can be seen that the proposed

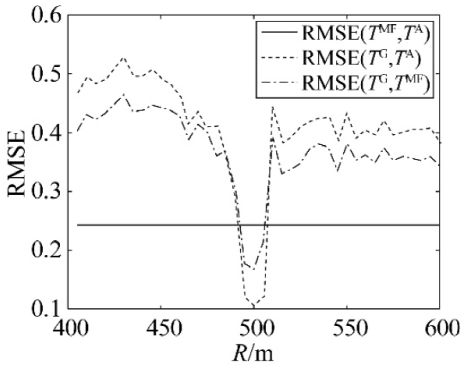

(a) RMSE between the reconstructed results T^{MF}, T^G and the target T^A

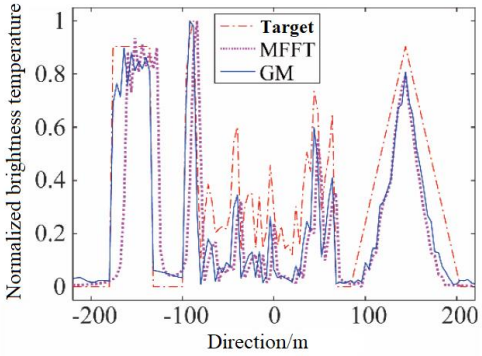

(b) Reconstruction results of the two imaging models (R_a = 500 m)

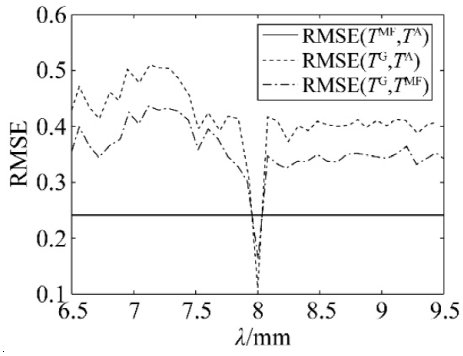

(c) Correction curves with respect to parameters λ (λ_a = 8 mm)

Figure 2. Simulation results.

correction method is also applicable to the correction of the parameters λ, which effectively verifies the feasibility of the proposed parameter correction method.

3.2 Estimation of real millimeter wave images

The parameter accuracy of the imaging model can be effectively improved by the above-mentioned parameter correction method, and then high-precision imaging inversion can be achieved by the regularization method. The advantage of the regularization method is that certain prior information is used to construct the regular term, which not only turns the pathological problem into a well-conditioned problem, but also can effectively improve the accuracy of reconstructed images. However, the regular terms used in the traditional regularization methods (e.g., equation (11)) are mostly quadratic convex functions, which smooth the image edges while causing parasitic ripples and edge blurring in the images. Therefore, to further improve the accuracy of the reconstructed image, this paper adopts the following improved regularized inverse model for image reconstruction with the idea of Total Variational (TV) parametrization:

$$\min_T J(\boldsymbol{T}) = \| \boldsymbol{GT} - \boldsymbol{V} \|_2^2 + \alpha P(\boldsymbol{T}) \tag{13}$$

$$P(\boldsymbol{T}) = \sum^{i,j \in \boldsymbol{T}} \{ | T(i,j) - T(i,j+1) | + | T(i,j) - T(i+1,j) | + | T(i,j) - T^{\mathrm{MF}}(i,j) | \} \tag{14}$$

where $P(T)$ is the improved regularization term, the first two terms of which are the TV parametrization, and it has been shown that using the TV parametrization as the regularization term can achieve more accurate image reconstruction results. In addition, given the high stability of the MFFT inversion results, the reconstructed image can be evaluated instead of the actual millimeter wave image; we introduce its reconstruction result TMF into the regularization term $P(T)$ to constrain the regularized reconstruction process and further improve the recovery accuracy. In this paper, the fast gradient projection FGP algorithm[8] is used to solve the optimization problem of equation (13), with the maximum iteration step k set to 20 and the parameter α set to 0.07.

The key of the proposed DM inversion method is to first perform parameter correction for the higher accuracy GM model to optimize its model accuracy; and then use an improved regularization method to reconstruct a high accuracy millimeter wave image. Since both the MFFT model and the GM model are based on the near-field integrated aperture imaging principle, the proposed DM inversion method is applicable to both near-field and far-field cases.

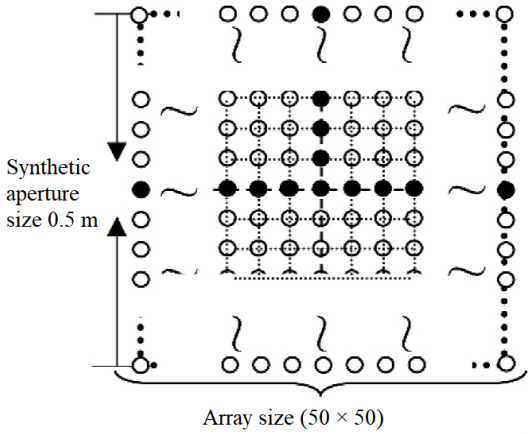

Figure 3. "T" array antenna distribution map.

4. Experiments and results

In this section, two typical target scene experiments are used as examples to simulate and analyze the proposed DM inversion method. The main simulation parameters are set the same as in **Table 1**. Considering that the MFFT inversion method requires a complete visibility function, a "T" type antenna array is used in the two-dimensional simulation, and its array elements are arranged as shown in **Figure 3**, with the real array elements (●) arranged along the axis and the corresponding visibility sampling points (○) uniformly distributed on the rectangular array surface.

The bright temperature image distribution of the target scene is shown in **Figure 4**, with dimension 100 × 100. To simulate the SAIR imaging process more faithfully, the simulation treats each pixel point in **Figure 4a** and **4b** as a discrete radiation source, its grayscale value as the radiation intensity, and the neighboring radiation source spacing is set to half of the system spatial resolution.

The signal received by the array antenna is obtained by integrating the millimeter wave radiation signal generated by all discrete point sources. Then the visibility function is derived by the complex correlation calculation between antenna pairs. After that, the MFFT method, TV regularization method and DM inversion method are used to reconstruct the image of the target scene respectively, where the parameters of MFFT method and TV regularization method are set as simulation parameters; the reconstruction results are shown in **Figure 5** and **Figure 6**.

(a) Tank and car scene

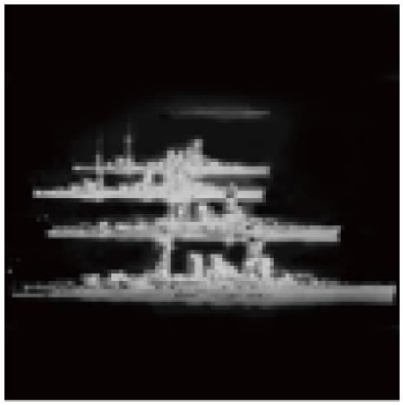

(b) Ship scene

Figure 4. Brightness temperature image distribution of the target scene.

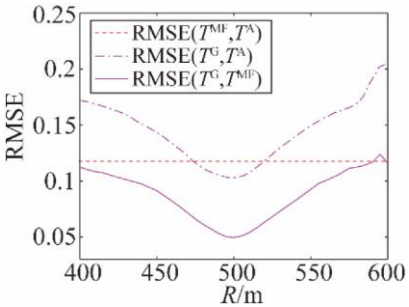

(a) Error curve RMSE (Ra = 495 m)

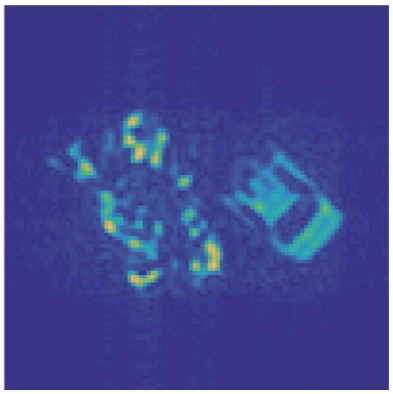

(b) MFFT method results

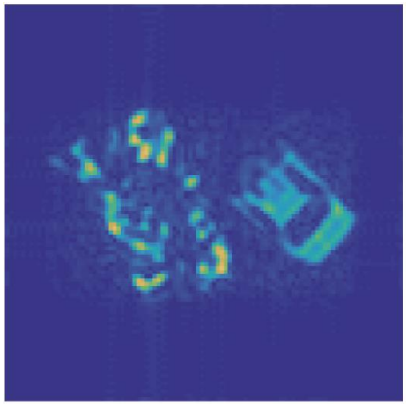

(c) TV method results

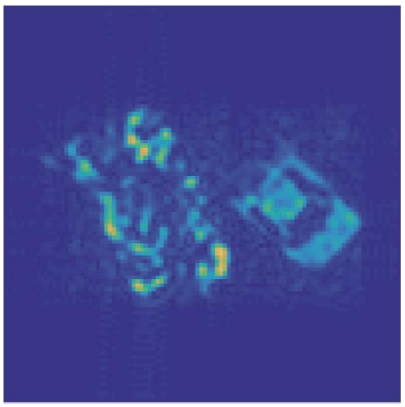

(d) DM method results

Figure 5. Inversion results of tank and car scenes.

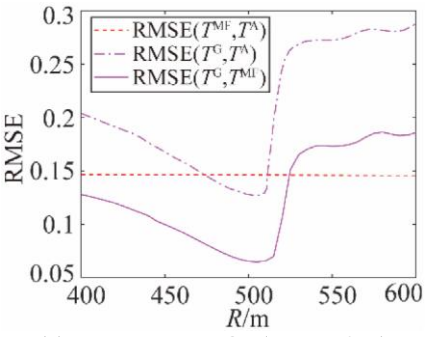

(a) Error curve RMSE (Ra = 510 m)

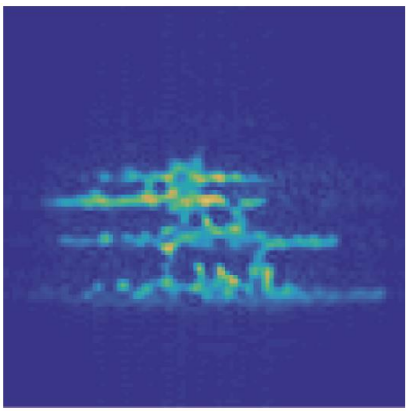

(b) MFFT method results

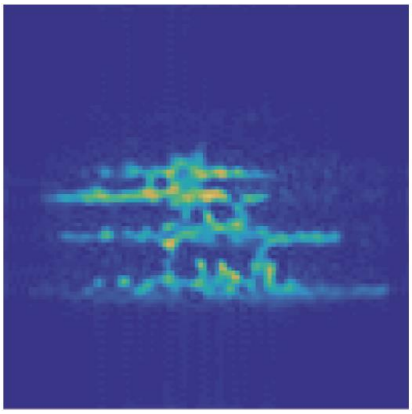

(c) TV method results

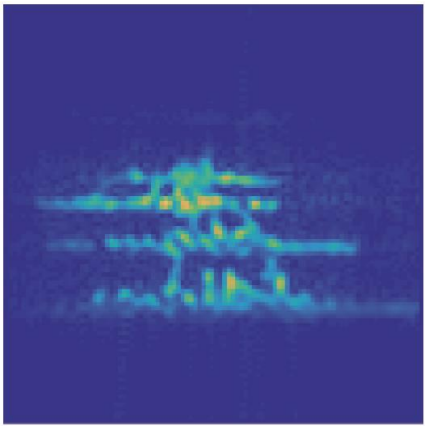

(d) DM method results

Figure 6. Inversion results of boat scenes.

From **Figure 5** and **Figure 6a**, it can be seen that the RMSE(T^{G},T^{A}) is smaller than RMSE(T^{MF},T^{A}) when the parameters R are close to the exact parameters, but higher than RMSE(T^{MF},T^{A}) for the parameters R with larger errors. In addition, since the GM model still has subtle model errors, the parameters R_a corresponding to the minimum values of RMSE(T^{G},T^{A}) and RMSE(T^{G},T^{MF}) are not exactly equal to the simulation parameters (R_a = 495 m in the tank scenario and R_a = 510 m in the ship scenario) in order to fit the model itself in a large number of 2D data inversions; therefore, it is necessary to perform model parameter correction with the proposed DM method for practical applications.

From the reconstruction results shown in **Figure 5b** and **Figure 6b**, it can be seen that there is a large noise pollution in the reconstructed images due to the low accuracy of the MFFT model and the fact that the Fourier transform also cannot effectively remove the image noise. In contrast, the GM matrix model has better model accuracy, and its inverse image accuracy (**Figure 5** and **Figure 6c**–**6d**) is significantly better than that of the MFFT image. In addition, the proposed DM inversion method uses an improved regularization term to constrain the regularization process, which can effectively improve the convergence speed of the image algorithm, and its reconstructed image (**Figure 5**, **Figure 6d**) has better accuracy than the traditional TV method with lower noise pollution. In order to objectively evaluate the accuracy of the reconstructed images, the peak signal-to-noise ratio (PSNR) and structural similarity ratio (SSIM) are calculated, and the results are shown in **Table 2**; obviously, the DM method inversion results have the smallest RMSE and the largest PSNR and SSIM. The results indicate that the proposed DM method can effectively correct the imaging model parameters and thus improve the imaging inversion accuracy of the integrated aperture radiometer.

5. Conclusion

A dual-model DM integrated aperture inversion method is proposed to address the problem that it is difficult to effectively perform image inversion based on a single-model imaging method when there is an error in the integrated aperture imaging model. The model parameters are corrected by comparing the reconstruction errors of the two models, and then the target scene is reconstructed with high accuracy by means of an improved regularization method. The simulation results show that the proposed DM method can effectively correct the imaging model parameter errors and reconstruct the target scene with high accuracy in millimeter wave images.

Table 2. Comparison of evaluation data of reconstructed images

Scene	Inversion method	Evaluation index		
		RMSE	PSNR	SSIM
Tank and vehicle	MFFT	29.1263	18.3577	0.8604
	TV	26.7083	18.9780	0.8764
	DM	25.5480	19.3243	0.8832
	MFFT	33.1131	17.1188	0.8384
Vessel	TV	29.6395	17.9660	0.8495
	DM	29.1390	18.0715	0.8601

Conflict of interest

The authors declare that they have no conflict of interest.

References

1. Zhang X, Gao Z, Li S. Zonghe kongjing wuyuan chengxiang tance xitong zhenlie texing fenxi (Chinese) [The characteristic of antenna array of passive synthetic aperture imaging system for target detection]. Journal of Microwaves 2018; 34(2): 56–60.
2. Miao J, Zheng C, Hu A, *et al*. Beidong haomibo shishi chengxiang jishu (Chinese) [Real-time passive millimeter wave imaging technology]. Journal of Microwaves 2013; 29(S1): 100–112.
3. Martin-Neira M, LeVine D, Kerr Y, *et al*. Microwave interferometric radiometry in remote sensing: An invited historical review. Radio Science 2014; (49): 415–449.
4. Chen J, Li Y, Wang J, *et al*. An accurate imaging algorithm for millimeter wave synthetic aperture imaging radiometer in near-field. Progress in Electromagnetics Research-Pier 2013; (141): 517–535.
5. Zhou X, Sun H, He J, *et al*. NUFFT-based iterative reconstruction algorithm for synthetic aperture imaging radiometers. IEEE Geoscience and Remote Sensing Letters 2009; 6(2): 273–276.
6. Feng L, Li Q, Chen K, *et al*. The gridding method for image reconstruction of nonuniform aperture synthesis radiometers. IEEE Geoscience and Remote Sensing Letters 2015; 12(2): 274–278.
7. Wu J, Zhang C, Liu H, *et al*. Performance analysis of circular antenna array for microwave interferometric radiometers. IEEE Transactions on Geoscience and Remote Sensing 2017; 55(6): 3261–3271.
8. Beck A, Teboulle M. Fast gradient-based algorithms for constrained total variation image denoising and deblurring problems. IEEE Trans Image Process 2009; (18): 2419–2434.